Geophys. J. R. astr. Soc. (1975) **41**, 51–63.

Spectral Characteristics of the L_g wave Generated by Central United States Earthquakes

Ronald L. Street*, Robert B. Herrmann† and Otto W. Nuttli

(Received 1974 November 30)‡

Summary

Spectra of more than three hundred short-period, vertical component L_g waves of 78 earthquakes in the central United States were determined. From these an empirical relationship between the long-period level of the L_g spectrum and the seismic moment was developed. The shape of the reduced spectrum shares some characteristics of Aki's revised model A. There is a uniform relationship between the corner period and the seismic moment, which implies a uniformity of earthquake processes in the central United States over a wide range of event sizes, as opposed to California where wide variations in the corner frequency are observed for source spectra having the same seismic moment. Using the reduced spectra, a method for relating magnitude observations at periods other than 1 s to m_b is outlined.

Introduction

Recent developments have led to better understanding of the seismic source. Early field and aftershock studies provided information on the fault area and average dislocation, and consequently the seismic moment (Brune & Allen 1967). Later Wyss & Brune (1968) developed an empirical relationship between the area beneath the coda envelope of a seismogram and the seismic moment. Aki (1967, 1972) proposed several models for the seismic source spectrum which accounted for far-field observations of the seismic moment, M_S vs m_b relationships, and other measurable properties of earthquakes. Aki's models provided initial estimates of the nature of the seismic source spectrum.

Brune (1970, 1971) assumed an instantaneous rupture on a circular fault plane and used the parameters of source dimension, fractional stress drop, and seismic moment to specify the shape of the far-field *S*-wave spectra. Thatcher & Hanks (1973) applied Brune's theory to a study of earthquakes in southern California. Trifunac (1972) and Hanks & Wyss (1972) modified Brune's theory in order to derive source parameters from *P*-wave spectra.

For many earthquakes the *S* phase is not a distinct arrival, but is associated with other arrivals of body- and surface-waves. The theory of Brune (1970, 1971) and work by Savage (1972) have not approached the problem of estimating source parameters

* Present address: Weston Geophysical Research, Inc., P.O. Box 550, Westboro, MA 01581

† Present address: Post-Doctoral Fellow, CIRES, University of Colorado, Boulder, CO 80302

‡ Received in original form 1974 September 3

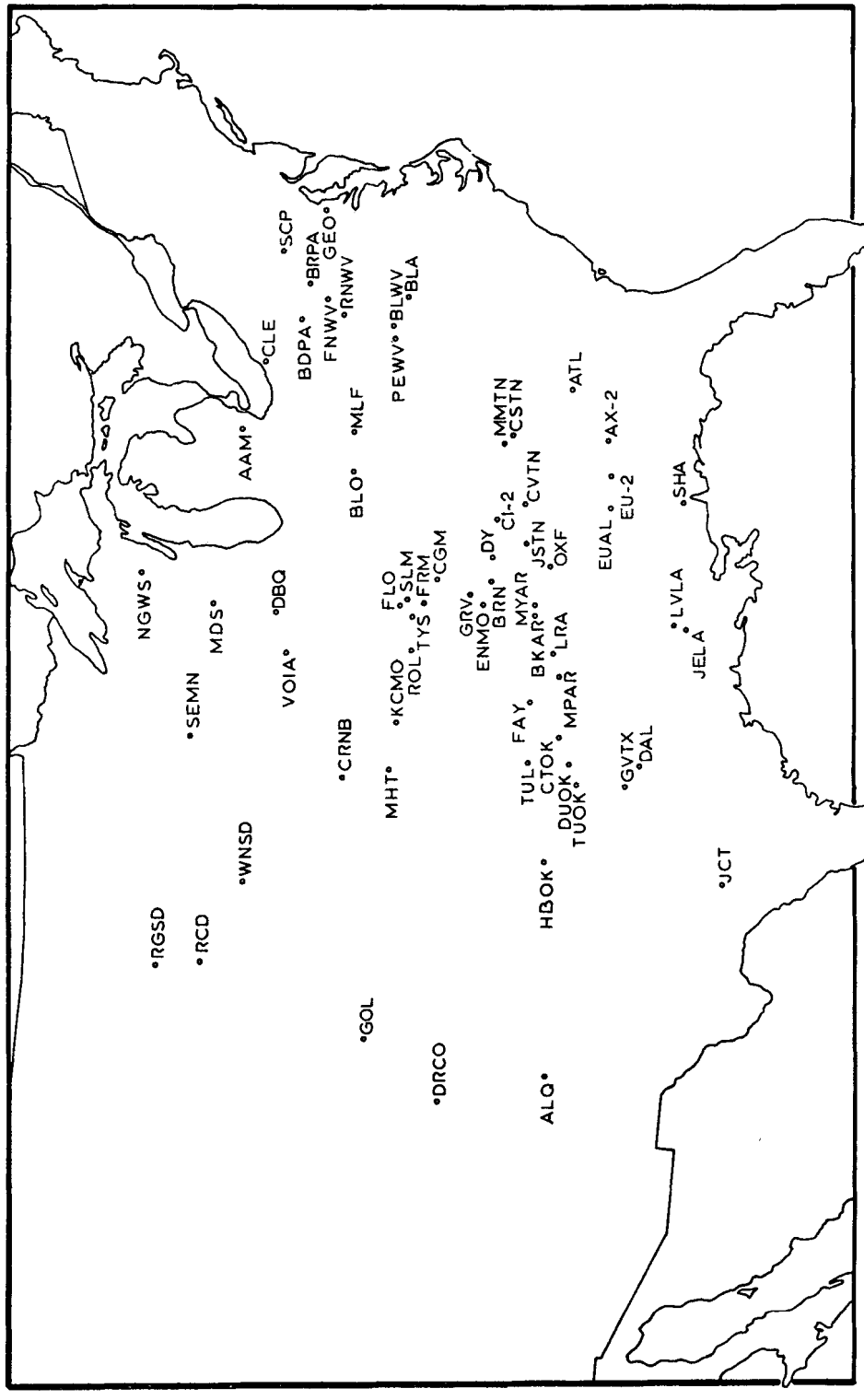

FIG. 1. Location of seismograph stations used for the short-period, vertical-component L_g spectral analysis.

from such a complicated set of arrivals. The objective of this paper is to accomplish this task.

Data analysis

The events studied occurred in the central United States between 1961 and mid-1974. The m_b magnitudes of these events fell between 0·5 and 5·0. For the smaller events, spectral observations were available from only one station, whereas for larger events up to ten spectral observations were made for an individual earthquake. The 63 seismograph stations which provided L_g observations at various times are shown in Fig. 1. These stations were part of the WWSSN, LRSM, Saint Louis University, or independent networks.

The instrument responses of the short-period vertical instruments varied from station to station. Fig. 2 illustrates some typical instrument responses used. This figure contains the familiar response curves of the WWSSN and LSRM networks together with the response of a magnetic tape recording system at FRM, Flat River, Missouri. To avoid undue amplification of noise at frequencies away from the pass band of the system, the suggestion of Berckhemer & Jacob (1970) was followed. The instrument-corrected spectra of the ground motion were used for analysis only in a pass band for which the instrument response was greater than one-tenth the maximum response.

In digitizing the seismograms, the magnetic tape system offered the best time resolution. The LSRM short-period seismograms, when viewed through a 10× viewer, were recorded at a rate of 150 mm min^{-1} whereas the WWSSN seismograms were recorded at a rate of 60 mm min^{-1}. The LRSM seismograms gave good spectral results at periods as short as 0·1 s, while the WWSSN data were useful only down to

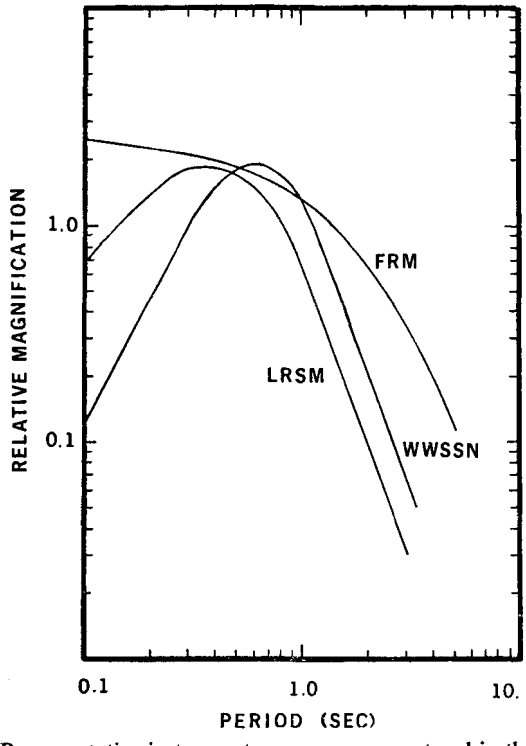

FIG. 2. Representative instrument responses encountered in this study.

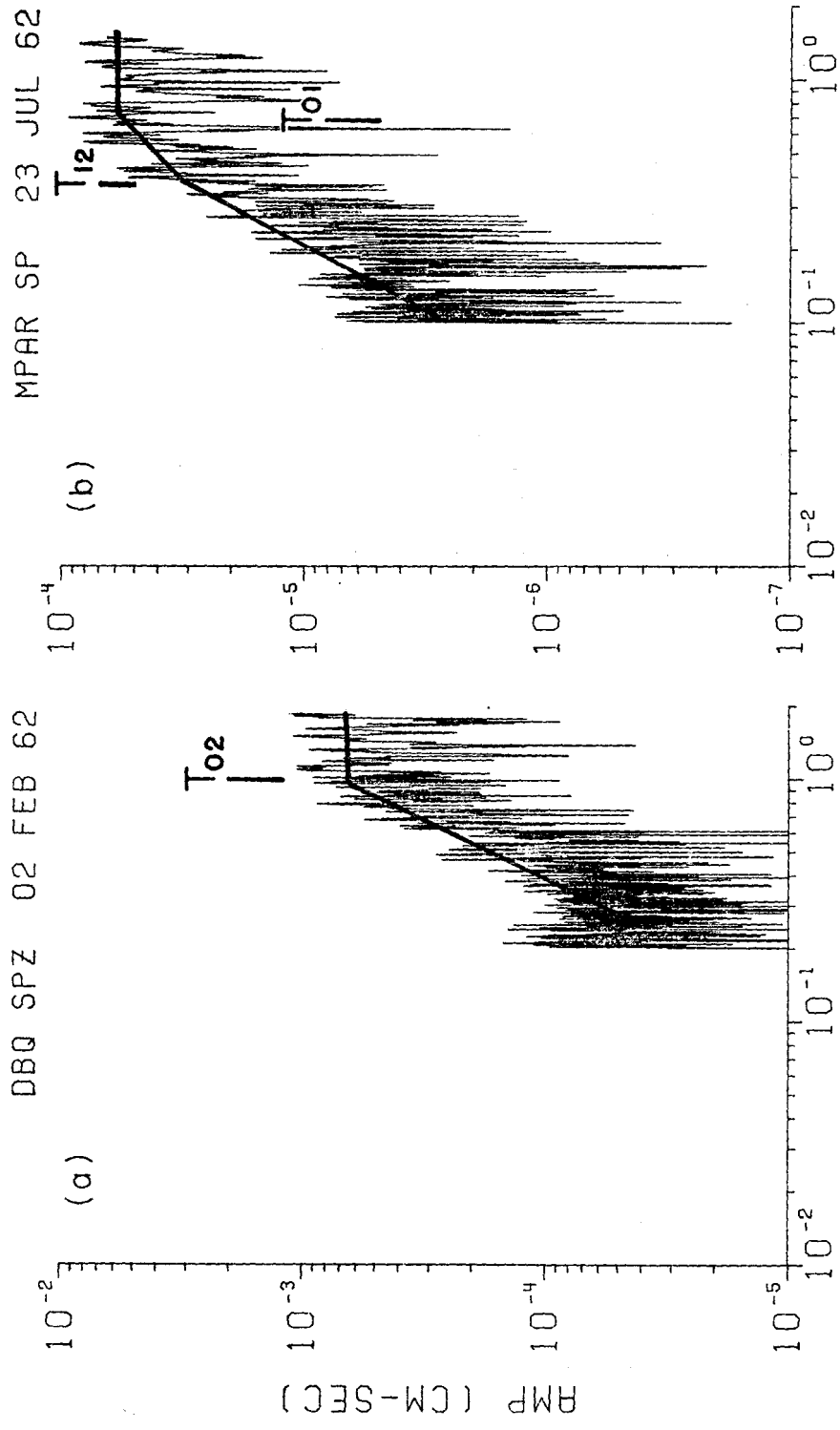

FIG. 4. (a) Event 3, 1962 February 2, showing the T_{02} corner between the ω^0 and ω^{-2} asymptotic trends of the spectra. (b) Event 6, 1962 July 23, showing the T_{01} corner between the ω^0 and ω^{-1} trends and the T_{12} corner between the ω^{-1} and ω^{-2} trends.

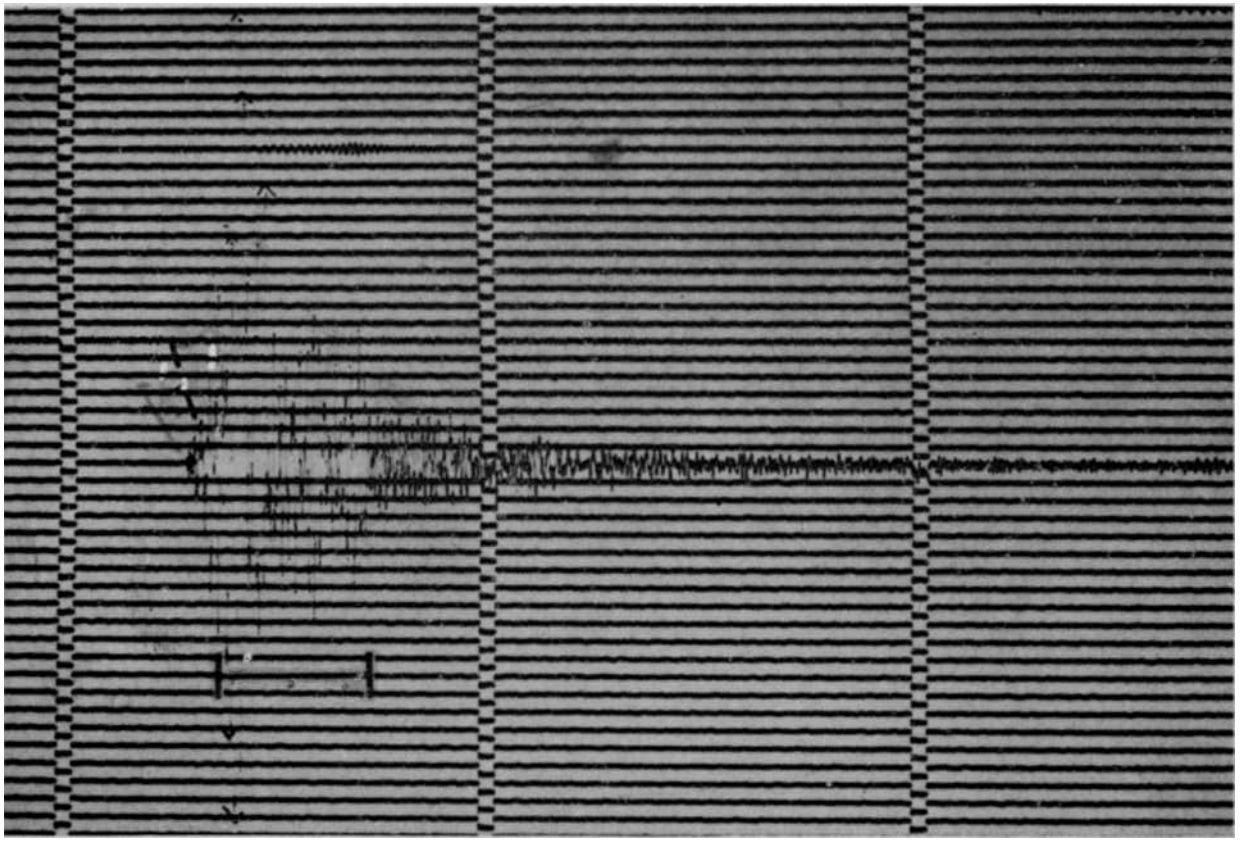

FIG. 3. Event 23 recorded at CGM, a distance of 24 km. The bar indicates the length of the record digitized, about 20 s.

(*facing p. 54*)

periods of 0·3 s. In general, the ground motion spectra from the same event recorded at different stations agreed very well, even though the various spectra may have been derived from different instrument systems.

A typical seismogram and time window used are shown in Fig. 3. The record was digitized from the time of the maximum trace offset, associated with the S_g or L_g arrival, until the signal reached the background noise level. For some events, the complete L_g wave train could not be digitized, due to magnetic tape saturation or loss of the photographic trace due to rapid high amplitude motion of the beginning of the L_g arrival. In such a case, it was found that if only the first 10–30 s were missing in the digitized seismogram, the resultant spectrum could be used for the location of the corner periods, although not for the determination of the seismic moment.

Sample displacement spectral densities are shown in Fig. 4. In this figure, the ground motion spectral densities (cm s) are plotted versus the period (s). A study of the two spectra contained in this figure leads to several observations. For both events, the spectrum is flat at the long-period end. On the other hand, ignoring the flatness at very short-periods, the L_g spectrum falls off with decreasing period, T, as T^2 (or ω^{-2}, where ω is the angular frequency). For some events, such as that of 1962 July 23, an intermediate ω^{-1} trend was observed. The ω^0, ω^{-1}, and ω^{-2} asymptotic trends of the spectra are indicated in Fig. 4 by the heavy straight lines.

The effect of anelastic attenuation upon the determination of the seismic moment and the choice of the corner frequencies was considered. Nuttli (1973) found a value of 6×10^{-4} km^{-1} for the anelastic attenuation coefficient γ of the 1 s L_g wave in the central United States. Because of the low attenuation, the maximum error in neglecting this effect would only be a factor of 3 at a distance of 1600 km for the 1-s period spectral components. Most of the observations were made at distance less than 500 km from the source, in which case the correction would be negligible. This is the period at which the ω^0 level, and hence the seismic moment, were set. Events with corner periods near 1 s would not exhibit much variation in the experimentally determined corner period for the same reason. Very small events, with corner periods near 0·1 s, were only recorded by stations within 50 km of the source, for which the anelastic attenuation corrections are again negligible. For these reasons, it was felt that neglect of the anelastic attenuation correction would not substantially affect the results.

Development of the empirical relationship

The similarity of the shape of the L_g spectrum, Fig. 4, with that predicted by Brune (1970) was noted early in the study. However, direct interpretation of the spectra according to Brune's (1970) theory did not seem valid since the L_g spectra were obtained from the vertical rather than the tangential component of motion, because the range of distances over which the spectra were studied no longer seemed adequate for the application of body-wave theory for an infinite medium, and because the L_g arrival is not a clear S phase but most likely a superposition of higher-mode surface waves and scattered waves.

The approach taken was to look for a relationship which properly corrected the L_g spectrum for geometrical spreading and at the same time related the long-period flat portion of the spectrum to the seismic moment M_0. As a starting point we used the relation of Keilis-Borok (1960) between the seismic moment M_0 of a double-couple seismic source and the far-field long-period spectral level of the S wave, Ω_0:

$$M_0 = 4\pi\rho\beta^3 r\Omega_0 R_{\theta\phi}^{-1}, \quad (1)$$

where ρ is the density, β is the shear-wave velocity, $R_{\theta\phi}$ is the S-wave radiation pattern, and r is the distance from the source. This formula is valid only for a shear-wave source in an infinite medium. Thatcher & Hanks (1973), in their study of SH spectra, adapted equation (1) to a half-space situation by accounting for the twofold

Table 1

Choice of r_0

Date	OT(UT)	Station	r (km)	Moment estimate $r_0=$ 20 km	$r_0=$ 100 km	$r_0=$ 200 km	T_{02} (s)
1965 March 6	21 08 51	GRV	80	9·2E20	1·8E21	1·8E21	0·6
		SLM	147	1·1E21	2·4E21	2·9E21	
		MHT	515	8·2E20	1·8E21	2·6E21	0·65
		DBQ	559	1·1E21	2·4E21	3·5E21	
		MDS	661	5·4E20	1·2E21	1·7E21	
		GVTX	742	4·9E20	1·1E21	1·5E21	
		ATL	761	6·6E20	1·5E21	2·1E21	
		BLWV	876	1·1E21	2·3E21	3·3E21	
		BRPA	1099	6·0E20	1·3E21	1·9E21	
1971 June 30	05 08 24	DY-4	40	4·5E19	5·9E19	5·9E19	0·20
		DY-5	40	4·6E19	6·0E19	6·0E19	0·17
		GRV	73	2·5E19	5·2E19	5·2E19	0·15
		FRM	152	3·0E19	6·0E19	8·4E19	0·23

increase in the amplitude of an *SH* wave at the free surface. This correction is theoretically valid only for *SH*-type motion and not the vertical motion of the *SV* wave.

Because of the complexity of the L_g wave train, it was decided to use equation (1) only as a guide in establishing the following empirical relationship, which relates the observed L_g spectrum $\Omega(\omega)$ at a distance r from the source to the distance corrected far-field estimate of the source spectrum $S(\omega)$:

$$S(\omega) = \begin{cases} 4\pi\rho\beta^3 r_0 (r/r_0)\, \Omega(\omega) & r \leqslant r_0 \\ 4\pi\rho\beta^3 r_0 (r/r_0)^{\frac{1}{2}}\, \Omega(\omega) & r \geqslant r_0. \end{cases} \tag{2}$$

Here r_0 serves two functions. First, if it is decided to restrict ρ and β to reasonable values for the medium, r_0 adjusts the scaling so that $S(\omega = 0) = M_0$. Secondly, r_0 establishes a distance which marks the change in the character of the geometrical spreading of the L_g wave train from that of typically body-wave at near distances to typically surface-wave at large distances. Note that the value of r_0 has no real physical significance, only an empirical one. A radiation pattern term has not been included since the later portions of the L_g train are composed primarily of scattered waves, which averages out the radiation pattern effects.

The values finally adopted for the parameters in equation (2) were $\rho = 2{\cdot}5\ \mathrm{g\,cm^{-3}}$, $\beta = 3{\cdot}5\ \mathrm{km\,s^{-1}}$, and $r_0 = 100\ \mathrm{km}$. Table 1 shows the effect on the seismic moment estimate by using other values for r_0. The table also gives the values of the corner period T_{02} for each event to indicate the consistency in the corner period determinations. The data for the 1965 March 6 event shows a variation of about a factor of two between the smallest and largest seismic moment estimates for each choice of r_0. However, the choice of $r_0 = 100\ \mathrm{km}$ shows slightly less variation between the largest and smallest estimates than the other choices of r_0. For the 1971 June 30 event, the seismic moments estimated from data at short epicentral distances, r, are greater than those estimated for large epicentral distances for the particular choice of $r_0 = 20\ \mathrm{km}$. For $r_0 = 200\ \mathrm{km}$, just the opposite occurs. Therefore, $r_0 = 100\ \mathrm{km}$ represents a reasonable compromise.

To test the appropriateness of the values for ρ, β, and r_0 in estimating the seismic moment, the seismic moments estimated from the L_g spectrum by using equation (2) are compared in Table 2 with the determinations made by Herrmann (1973, 1974) from a study of the long-period, fundamental surface-wave excitation by nine central

Table 2

Comparison of seismic moment estimates

Date	M_0* dyne-cm	M_0† dyne-cm	Number observations
1962 February 2	2·6E22	2·0E22	1
1963 March 3	7·7E22	7·5E22	2
1965 August 14	1·4E21	1·7E21	4
1965 October 21	6·9E22	7·0E22	5
1967 July 21	1·2E22	9·0E21	2
1969 January 1	3·8E22	3·7E22	1
1970 November 17	1·1E22	1·2E22	4
1972 September 15	1·7E22	1·7E22	4
1973 November 30	1·0E22	1·2E22	4

* Long-period surface wave determinations (Herrmann 1974)

† L_g estimates (equation (2))

and eastern United States earthquakes. The agreement is excellent in view of an estimated multiplicative error of 1·5 in the surface-wave seismic moment determinations (Herrmann 1974).

L_g spectral character

Equation (2) was applied to the spectra obtained from 78 earthquakes in the central United States. For each event average values of the seismic moment and corner periods were determined from the distance corrected spectra. The pertinent parameters for each event are summarized in Table 3. This table contains an identification number, date, origin time, epicentral co-ordinates, mean seismic moment estimate, number of observations, corner-periods, and magnitude for each earthquake. In Table 3, the column headed by T_{01} represents the corner-period between the ω^0 and ω^{-1} asymptotic trends of the source spectrum. T_{12} is the corner-period between the ω^{-1} and ω^{-2} trends and T_{02} is the corner-period between the ω^0 and ω^{-2} trends. For many events there was only a T_{02} corner-period. For events having T_{01} and T_{12} corners, a T_{02} corner-period is defined as the geometrical mean of T_{01} and T_{12}; these T_{02} are enclosed in parentheses.

Table 3 was used to plot Fig. 5, which is a sketch of the general features of the L_g source spectra estimates. Fig. 5 conatins the ω^0, ω^{-1}, and ω^{-2} asymptotes from some representative events. The number to the right of each spectrum refers to the event number in Table 3. It is interesting to note that for events with seismic moments less than 10^{20} dyne cm, no ω^{-1} trend was observed. For events with greater seismic moments, ω^{-1} trends were noted at times.

Fig. 6 is a plot of the T_{02} corner period versus the seismic moment. The average trend of the corner-period is indicated by the straight line segments. Several interesting features are seen in this plot. First, there is a consistent relationship between the corner-period and the seismic moment. A similar relationship has not been found in southern California, where wide ranges in stress drop introduce a wide variation in corner-periods for a given seismic moment value (Thatcher & Hanks 1973). The kink in the corner-period is a characteristic of Aki's (1972) revised model A. On the other hand, the relationship of the seismic moment to the cube of the corner-period, in regions excluding the kink, is a characteristic of Aki's (1972) models A and B, but not of his revised model A.

Brune (1970, 1971) derived an expression for the far-field spectrum of the *SH* wave from a source in an infinite medium. He related the corner-period T_{02} to the source dimension and found that under the conditions of constant stress drop there is a relationship between the seismic moment and the cube of the corner-period.

Table 3

Earthquake source parameters

Event	Date	UT(OT)	Lat °N	Long °W	M_0	Num obs	Corner periods (s) T_{01}	T_{02}	T_{12}	m_b
1	1961 December 25	12 20 03	39·1	94·6	4·0E20	2				
2	1961 December 25	12 58 21	39·1	94·6	3·6E20	2				
3	1962 February 2	06 43 34	36·6	89·7	2·0E22	5		1·0		4·3
4	1962 June 1	11 23 41	36·0	90·2	2·5E20	9	0·7			3·2
5	1962 July 14	04 23 49	36·5	89·9	5·8E20	10		0·6		3·2
6	1962 July 23	06 05 17	36·1	89·4	1·4E21	9	0·8	(0·55)	0·4	4·2
7	1963 March 3	17 30 13	36·7	90·0	7·5E22	2		1·3		4·7
8	1963 March 31	13 31 04	36·9	89·0	6·0E19	3		0·6		3·0
9	1963 April 6	08 12 22	36·5	89·6	2·0E20	7		0·4		3·1
10	1963 August 3	00 37 48	37·0	88·7	3·0E21	10	1·0	(0·85)	0·75	4·0
11	1964 January 16	05 09 57	36·8	89·5	4·4E20	6	0·6	(0·46)	0·35	3·0
12	1964 March 17	02 16 06	36·2	89·6	1·8E20	7		0·55		3·5
13	1964 May 23	11 25 34	36·6	90·0	1·8E21	6	0·7	(0·50)	0·35	4·0
14	1964 May 23	15 00 34	36·6	90·0	2·4E20	3				3·5
15	1965 February 11	03 40 24	36·4	89·7	5·3E20	9	0·55	(0·40)	0·3	3·5
16	1965 March 6	21 08 51	37·5	91·1	1·8E21	9	0·6			4·1
17	1965 March 25	12 59 28	36·4	89·5	3·0E21	13	0·85	(0·55)	0·35	3·7
18	1965 August 14	05 04 30	37·2	89·3	2·3E20	7		0·35		2·9
19	1965 August 14	05 46 18	37·2	89·3	2·5E20	6		0·4		3·2
20	1965 August 14	05 59 27	37·2	89·3	2·9E19	2		0·22		2·5
21	1965 August 14	13 13 56	37·2	89·3	1·7E21	5		0·55		3·8
22	1965 August 15	04 19 01	37·2	89·3	2·6E20	6		0·35		3·5
23	1965 August 15	06 07 28	37·2	89·3	4·0E20	4		0·4		3·4
24	1965 August 15	11 19 38	37·2	89·3	3·0E19	3		0·17		2·7
25	1965 October 21	02 04 38	37·5	91·1	7·0E22	7	2·0	(1·4)	1·0	4·9
26	1965 November 4	07 43 33	37·1	91·0	1·0E21	7	0·8	(0·55)	0·4	3·8
27	1966 February 12	04 32 15	35·9	90·0	9·4E20	9	0·75	(0·60)	0·45	3·6
28	1966 February 13	06 29 43	33·6	87·0	3·0E21	4		0·75		3·5
29	1966 February 13	23 19 37	37·0	91·0	1·0E21	7		0·65		3·2
30	1966 February 14	00 08 56	37·0	91·0	2·2E20	5	0·52	(0·40)	0·3	3·1
31	1966 February 26	08 10 19	37·1	91·0	7·0E20	10		0·6		3·6
32	1966 December 6	08 00 47	38·8	92·8	2·0E20	3		0·5		2·9
33	1967 July 21	09 14 49	37·5	90·6	9·0E21	2	1·0			4·3
34	1967 August 5	11 37 31	38·3	90·6	1·0E20	3				2·8
35	1968 February 10	01 34 32	36·5	89·9	5·1E21	2	1·1	0·9	0·7	3·5
36	1969 January 1	23 35 36	34·8	92·6	3·7E22	1	1·7	(1·0)	0·6	4·5
37	1969 February 28	13 10 13	37·9	88·9	1·6E20	6		0·4		3·2

Table 3 (*continued*)

38	1970 March 27	03 44 29	36·5	89·7	1·5E20	5		0·3		3·5
39	1970 November 17	02 13 54	35·9	90·2	1·2E22	4	0·95	(0·53)	0·3	4·4
40	1970 November 30	04 46 53	36·2	89·9	2·8E20	2	0·45	(0·35)	0·3	2·8
41	1971 January 1	14 36 23	36·3	89·5	8·7E18	1		0·13		
42	1971 February 12	12 44 27	38·5	87·9	4·2E20	7	0·7	(0·5)	0·35	3·3
43	1971 April 7	03 43	35·9	90·2	1·8E19	3		0·15		
44	1971 April 13	14 00 50	35·7	90·1	1·2E20	7		0·15		2·8
45	1971 April 17	05 01 05	36·2	89·6	3·5E18	2		0·1		
46	1971 April 18	06 11 30	36·5	89·6	4·1E18	2		0·1		
47	1971 April 22	04 14 34	36·5	89·5	4·0E18	2		0·13		
48	1971 May 30	08 04 49	35·9	89·9	9·0E19	5		0·25		
49	1971 June 30	05 08 24	36·6	89·7	6·0E19	4		0·17		
50	1971 June 30	21 45 53	36·5	89·6	2·0E17	2		0·07		
51	1971 July 1	05 52	36·4	89·5	3·0E17	2		0·08		
52	1971 July 4	14 37 58	36·4	89·5	3·0E18	3		0·1		
53	1971 August 2	12 39 38	36·6	89·8	1·0E18	3		0·09		
54	1971 September 29	11 14 08	36·5	89·5	2·0E18	3		0·1		
55	1971 September 29	13 14 41	36·3	89·5	1·5E18	3		0·09		
56	1971 September 29	19 23 58	37·1	89·4	4·0E19	4		0·15		
57	1971 October 1	18 49 39	35·8	90·4	4·0E21	3	0·8	(0·55)	0·4	4·1
58	1971 October 7	08 31 10	36·0	90·0	3·6E19	2		0·17		
59	1971 October 8	10 42 54	36·5	89·6	2·2E18	3		0·08		
60	1971 October 18	06 39 31	36·7	89·6	1·0E20	4		0·5		3·0
61	1971 October 30	01 28 35	36·5	89·6	3·2E18	3		0·1		
62	1971 November 4	18 54 01	37·6	90·1	8·0E18	3		0·13		
63	1971 November 8	04 34 55	36·5	89·7	9·4E18	1		0·12		
64	1972 February 1	05 42 10	36·4	90·8	1·7E21	7	0·5			4·2
65	1972 March 29	20 38 32	36·2	89·6	2·0E21	3	0·8	(0·6)	0·5	3·7
66	1972 May 7	02 12 08	35·9	90·6	5·8E20	2	0·75	(0·6)	0·45	3·4
67	1972 June 8	16 49 49	36·2	89·6	2·6E17	1		0·07		
68	1972 June 19	05 46 15	37·0	89·1	2·2E20	6		0·5		3·2
69	1972 June 21	02 31 17	37·1	89·9	3·0E19	4		0·18		2·7
70	1972 September 15	05 22 15	41·6	89·3	1·3E22	4	0·75	(0·6)	0·45	4·4
71	1973 January 7	22 56 06	37·4	87·3	3·2E20	2				3·2
72	1973 January 12	11 56 56	37·9	90·5	1·2E20	2				
73	1973 October 3	03 50 20	35·7	90·1	3·6E20	3		0·6		3·4
74	1973 October 9	20 15 27	36·5	89·6	9·0E20	5	0·55			3·7
75	1973 November 30	07 48 41	35·8	84·0	1·2E22	7	1·0	(0·6)	0·35	
76	1974 January 8	01 12 37	36·2	89·4	3·0E21	4	0·7	(0·6)	0·54	4·0
77	1974 April 3	23 05 03	38·5	88·0	4·1E22	5	1·3			
78	1974 June 5	08 07 11	36·8	89·9	6·0E20	5		0·55		3·6

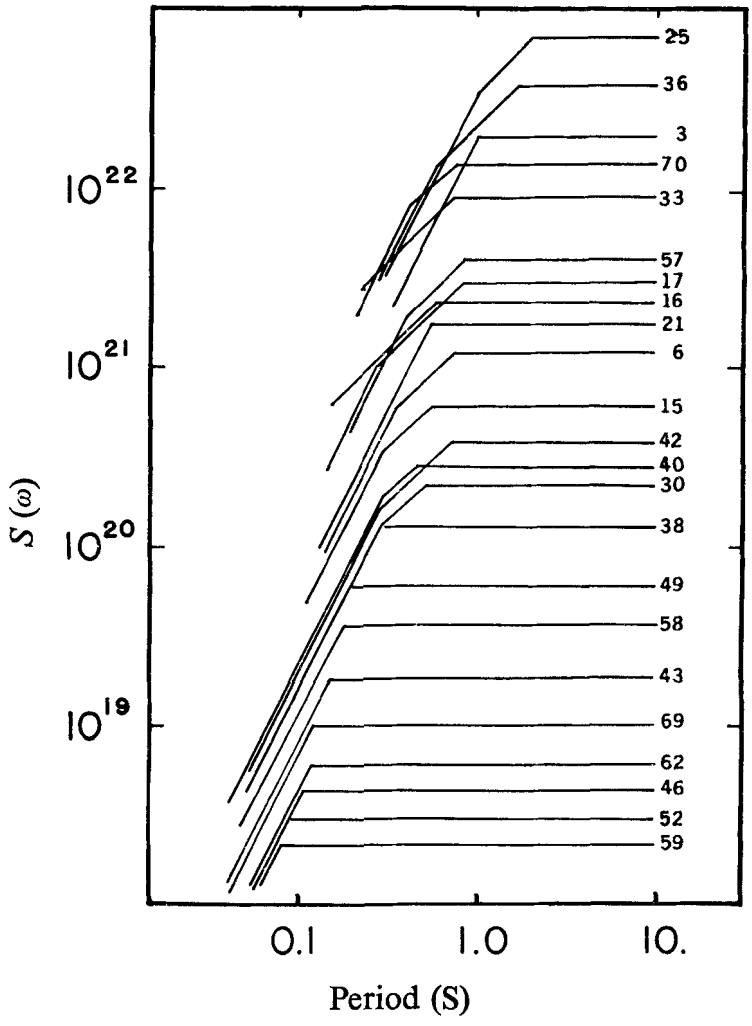

FIG. 5. General shape of the L_g estimated source spectra $S(\omega)$.

If we interpret our L_g spectra according to the relationships derived by Brune (1970, 1971), it is found that central United States earthquakes with seismic moments less than 10^{21} dyne cm are characterized by a constant stress drop of about 1 bar, whereas events with seismic moments between 5×10^{21} and 10^{23} dyne cm exhibit a constant stress drop of about 6 bars. The kink in Fig. 6 marks a transition between earthquakes with stress drops of 1 bar and 6 bars.

The shape of the reduced spectra shown in Fig. 5 can also be interpreted using Brune's (1970) terminology of partial and complete stress drop events. In Fig. 5, it is seen that events with seismic moments less than 3×10^{20} dyne cm exhibit only an ω^{-2}, or complete stress drop behaviour. Some of the larger events also exhibit an ω^{-1} trend, which is indicative of partial stress drop events.

Development of magnitude scales

The development of source spectrum models by Aki (1967, 1972) was based on known values of seismic moment, an assumption of the shape of the source spectrum,

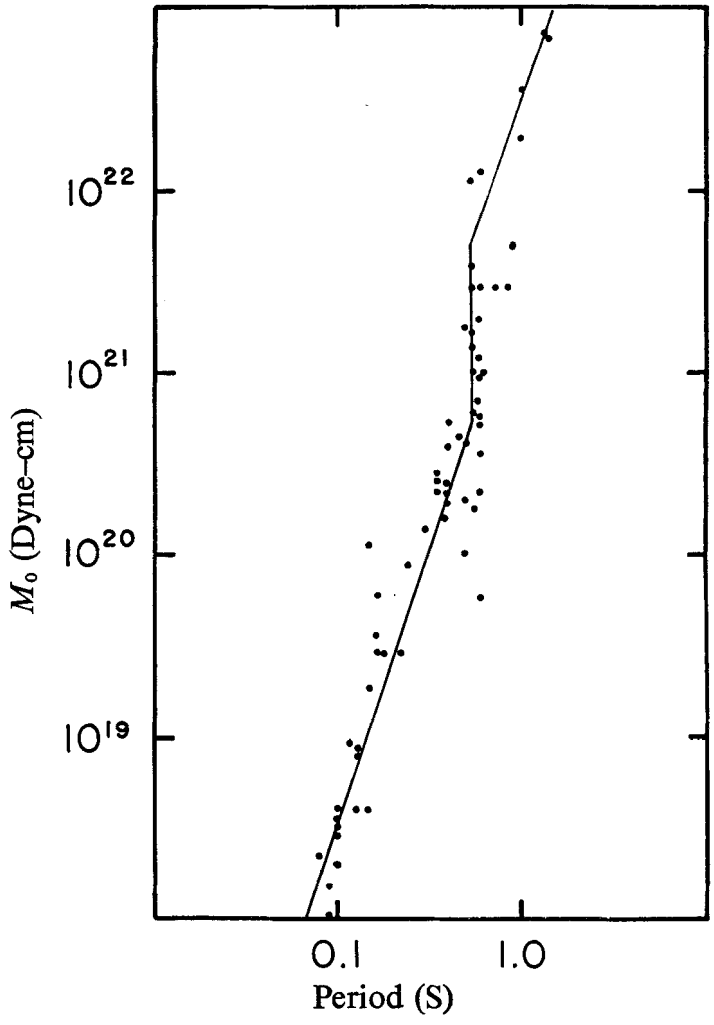

FIG. 6. Plot of the T_{02} corner period as a function of seismic moment.

and variation on the position of the corner-period as required by m_b vs M_S scaling. As the shape of the source spectrum, the seismic moments, and the M_S and m_b values are known for the set of central United States earthquakes studied, we can compare the M_0, M_S and m_b values with magnitude scales utilizing other wave periods. Thatcher (1973) considered the effect of source spectrum scaling upon the local magnitude M_L derived from different instrument systems. However, we use a magnitude definition based upon ground amplitudes, obtained by accounting for the particular seismograph response.

In general the equation for determining magnitude within a certain distance range of applicability is of the form (Nuttli 1972)

$$m_T = B(T)+C(T, D)\log_{10}(D)+\log_{10}(A/T) \quad (3)$$

where D is the epicentral distance and A is the maximum sustained ground displacement at period T of the given wave type. The coefficient C corrects for geometrical spreading and anelastic attenuation. The factor B scales the formula to some predetermined level.

Table 4

M_0 dyne-cm	M_S	m_b	$m_{0.3}$	$m_{0.1}$
10^{23}	4·2	5·0	(4·0)	(3·0)
10^{22}	3·2	4·5	(3·9)	(3·0)
10^{21}	2·2	3·2	3·3	2·4
10^{20}	1·2	2·5	2·5	1·8
10^{19}	0·2	1·5	1·5	1·5
10^{18}	−0·8	0·5	0·5	0·5

Assuming that the magnitude defined for a given period T is directly related to $\log_{10} S(\omega)$, a relationship between a magnitude scale at period T and some other period T' can be established by comparing the relative levels of the source spectrum at the two periods. For example, from Fig. 5, in comparing spectra with $M_0 = 10^{20}$ dyne cm to $M_0 = 10^{21}$ dyne cm, we would expect a 1·0 unit change in M_S (20-s period) and m_b (1-s period) and a 0·7 unit change in the magnitude $m_{0.3}$ based on a 0·3 s L_g component and a 0·7 unit change in $m_{0.1}$, a magnitude based on the 0·1-s period component.

To clarify this, assume that the $C(T, D)$ are known and that $B(T)$ have been specified such that $m_b = m_T$ at $T = 0{\cdot}3$ seconds and $T = 0{\cdot}1$ seconds for an $m_b = 1{\cdot}5$ earthquake. Using the L_g spectra of Fig. 5, the new magnitude scales are compared in Table 4. This table gives the correspondence between the values of M_0, M_S, m_b, $m_{0.3}$ and $m_{0.1}$. The table is scaled by using the observed M_0, M_S, and m_b values (underlined) for the 1963 March 3 and 1965 October 21 earthquakes. The $m_{0.3}$ and $m_{0.1}$ quantities in parentheses represent values for which the shape of the short-period source spectrum is not adequately known and an ω^{-2} trend is assumed.

Because of the predictability of source characteristics for the central United States earthquakes, as noted from Fig. 6, a reliable estimate of m_b can be made from signals with periods other than 1 s by using a relationship such as that found in Table 4. This is of importance since microearthquake studies usually record periods less than 1 s and this relationship will allow the consistency of using the same magnitude m_b.

Conclusions

A study of the vertical component L_g spectra has led to several new results. An empirical relationship has been developed to determine the seismic moment and the far-field estimate of the source spectrum shape from the L_g wave. The technique made use of observed L_g spectral data at a number of distances in order to determine the effect of geometrical spreading on the spectra. Known seismic moment values, in this case obtained independently from long-period, surface-wave studies, were used to scale the empirical relationship.

The shape of the source spectrum as estimated from the L_g spectra for central United States earthquakes is characterized by ω^0 and ω^{-2} trends for events with seismic moments less than 10^{20} dyne cm. For some events with greater seismic moments, an ω^{-1} trend was also observed. Events with seismic moments less than 10^{21} dyne cm exhibit constant stress drop behaviour with a stress drop of about 1 bar, whereas events with seismic moments greater than 5×10^{21} dyne cm have constant stress drops of about 6 bars. This relationship is so consistent as to suggest a uniformity of earthquake processes in the region as compared to southern California, where a wide range in stress drops occurs for events with the same seismic moment.

Finally, the observations of the L_g source spectra estimates were used to establish a relationship between m_b and magnitude scales based on periods other than 1 s. This will be of use in assigning m_b values to microearthquakes in the region.

Acknowledgments

This research has been sponsored in part by NSF Grant GA–40595 and AFOSR Contract F44620–73–C–0042. Mr James Zollweg of Saint Louis University provided the epicentral data and magnitudes for the events listed in Table 3. Thanks are extended to Dr T. C. Hanks for critically reading the manuscript and making helpful comments.

Department of Earth and Atmospheric Sciences,
Saint Louis University,
P.O. Box 8099 *Laclede Station,*
St Louis, MO 63156, *USA.*

References

Aki, K., 1967. Scaling law of seismic spectrum, *J. geophys. Res.*, **72,** 1217–1231.

Aki, K., 1972. Scaling law of earthquake source time-function, *Geophys. J. R. astr. Soc.*, **31,** 3–25.

Berckhemer, H. & Jacob, K. H., 1970. Investigation of the dynamical process in earthquakes by analyzing the pulse shape of body waves, *Proceedings of the X Assembly of the European Seismological Commission Leningrad* 3–11 *September* 1968, Vol. II, 253–333.

Brune, J. N., 1970. Tectonic stress and the spectra of seismic shear waves from earthquakes, *J. geophys. Res.*, **75,** 4997–5009.

Brune, J. N., 1971. Correction to ' Tectonic stress and the spectra of seismic shear waves from earthquakes ', *J. geophys. Res.*, **76,** 5002.

Brune, J. N. & Allen, C. R., 1967. A low stress-drop, low-magnitude earthquake with surface faulting: the Imperial, California, earthquake of March 4, 1966, *Bull. seism. Soc. Am.*, **57,** 501–514.

Hanks, T. C. & Wyss, M., 1972. The use of body-wave spectra in the determination of seismic source parameters, *Bull. seism. Soc. Am.*, **62,** 561–590.

Herrmann, R. B., 1973. Surface-wave generation by the south central Illinois earthquake of November 9, 1968, *Bull. seism. Soc. Am.*, **63,** 2121–2134.

Herrmann, R. B., 1974. *Surface wave generation by central United States earthquakes,* Ph.D. Dissertation, Saint Louis University.

Keilis-Borok, V. I., 1960. *Investigation of the mechanism of earthquakes, Sov. Res. Geophys.*, 4 (transl., *Tr. Geofis. Inst.*, **40,** 1957), 201 pp., American Geophysical Union, Consultants Bureau, New York.

Nuttli, O. W., 1972. Magnitude, intensity and ground motion relations for earthquakes in the central United States, *Proceedings of the International Conference on Microzonation for Safer Construction Research and Application, Seattle, Oct* 30–*Nov* 3, pp. 307–318.

Nuttli, O. W., 1973. Seismic wave attenuation and magnitude relations for eastern North America, *J. geophys. Res.*, **78,** 876–885.

Savage, J. C., 1972. The relation of corner frequency to fault dimensions, *J. geophys. Res.*, **77,** 3788–3795.

Thatcher, W., 1973. A note on discrepancies between local magnitude (M_L) and microearthquake magnitude scales, *Bull. seism. Soc. Am.*, **63,** 315–319.

Thatcher, W. & Hanks, T. C., 1973. Source parameters of southern California earthquakes, *J. geophys. Res.*, **78,** 8547–8576.

Trifunac, M. D., 1972. Stress estimates for the San Fernando, California, earthquake of February 9, 1971: Main event and thirteen aftershocks, *Bull. seism. Soc. Am.*, **62,** 721–750.

Wyss, M. & Brune, J. N., 1968. Seismic moment, stress and source dimensions for earthquakes in the California–Nevada region, *J. geophys. Res.*, **73,** 4681–4694.